

# Composition of Clusters and Building Blocks in Amylopectins from Maize Mutants Deficient in Starch Synthase III

Fan Zhu,<sup>†</sup> Eric Bertoff,<sup>‡</sup> and Koushik Seetharaman<sup>\*‡</sup>

<sup>†</sup>School of Chemical Sciences, University of Auckland, Private Bag 92019, Auckland 1142, New Zealand

<sup>‡</sup>Department of Food Science and Nutrition, University of Minnesota, 1334 Eckles Avenue, St. Paul, Minnesota 55108, United States

**ABSTRACT:** Branches in amylopectin are distributed along the backbone. Units of the branches are building blocks (smaller) and clusters (larger) based on the distance between branches. In this study, composition of clusters and building blocks of amylopectins from *dull1* maize mutants deficient in starch synthase III (SSIII) with a common genetic background (W64A) were characterized and compared with the wild type. Clusters were produced from amylopectins by partial hydrolysis using  $\alpha$ -amylase of *Bacillus amyloliquefaciens* and were subsequently treated with phosphorylase *a* and  $\beta$ -amylase to produce  $\varphi,\beta$ -limit dextrins. Clusters were further extensively hydrolyzed with the  $\alpha$ -amylase to produce building blocks. Structures of clusters and building blocks were analyzed by diverse chromatographic techniques. The results showed that the *dull1* mutation resulted in larger clusters with more singly branched building blocks. The average cluster contained  $\sim 5.4$  blocks in *dull1* mutants and  $\sim 4.2$  blocks in the wild type. The results are compared with previous results from SSIII-deficient *amo1* barley and suggest fundamental differences in the cluster structures.

**KEYWORDS:** *dull1* maize mutant, cluster structure, building block structure, amylopectin

## INTRODUCTION

Starch is composed of two macropolymers of glucose in the form of amylose and amylopectin. Amylose is essentially linear with  $\alpha$ -(1,4) linkages, whereas amylopectin is highly branched by  $\alpha$ -(1,6) bonds. Although the exact branching pattern of amylopectin is still to be established, models of the structure have been proposed. It was suggested that the branches in amylopectin are mostly distributed and scattered along a backbone consisting mainly of longer chains.<sup>1,2</sup> The branching zones, representing the internal part of the amylopectin, build up the amorphous lamellae in the starch granules. Based on a set of internal structural features, amylopectins from diverse botanical origins were categorized into four types.<sup>3</sup> Type 1 has the lowest amounts of long B-chains (a B-chain carries more than one other chain, as opposed to an A-chain, which carries only one other chain) and the highest amounts of short B-chains, whereas type 4 has the opposite proportion. Types 2 and 3 are intermediate between types 1 and 4. Previous studies showed that the structure of amylopectin is linked to that of their clusters and building blocks. The links can be explained by the backbone model of amylopectin.<sup>1,2</sup>

Structural units of groups of branches are building blocks and clusters depending on the distances between the branches. Clusters can be isolated by partial hydrolysis with the  $\alpha$ -amylase of *Bacillus amyloliquefaciens*, which has a high propensity for endoaction.<sup>4</sup> All amylopectins analyzed so far showed that the clusters, in the form of  $\varphi,\beta$ -limit dextrins or  $\beta$ -limit dextrins, have an average molecular size with a degree of polymerization (DP) in the range of  $\sim 60$ – $90$ .<sup>1</sup> Further, extensive  $\alpha$ -amylolysis of the limit dextrins of clusters produces tightly branched building blocks. These blocks can be categorized into groups based on the average number of chains per block.<sup>5</sup> Groups 2–4 contain two to four chains per block, respectively, whereas larger blocks in groups 5 and 6 have up to 10 or more chains.

All amylopectins analyzed so far showed that building blocks of group 2 are the most abundant ( $\sim 50\%$  by number). Systematic studies of the internal structures of amylopectins from different plant species revealed correlations between the internal unit chains, clusters, and building blocks.<sup>1–3</sup> Thus, isolated clusters from amylopectins with higher amounts of long B-chains also tend to have higher amounts of long chains and vice versa. However, more samples with diverse structures, especially mutants with altered structures, remain to be analyzed to obtain a more refined picture of the relations between the structures of amylopectin, clusters, and building blocks and the mechanism of starch biosynthesis.

Maize (*Zea mays* L.) is one of the most important crops, used in a wide range of applications in the food and nonfood industries, and its major component is starch. Maize starches modified by genetic means can represent novel properties to better suit specific applications.<sup>6</sup> Several known endosperm mutant genes in maize, such as *ae*, *sh1*, *du*, and *wx*, alter the properties of starch but have small effects on starch yield.<sup>7</sup> Analysis of mutant samples with detailed genetics presents an excellent opportunity to better understand biosynthesis–structure–property relationships for diverse applications. Amylopectin biosynthesis involves the soluble starch synthases (SSs), starch branching enzymes (BEs), and starch debranching enzymes (DBEs), and amylose synthesis involves granule-bound starch synthase I (GBSSI) encoded by the *waxy* gene in diverse plants.<sup>7</sup> Some of these biosynthetic enzymes form complexes in vivo and interact to synthesize starch in coordinative ways in diverse plants.<sup>8</sup> Altering the activity or

**Received:** August 30, 2013

**Revised:** November 13, 2013

**Accepted:** November 14, 2013

**Published:** November 14, 2013

presence of certain enzymes usually leads to changed expression levels of other enzymes.<sup>8–11</sup> Coordination of enzyme activities due to the protein–protein interactions in relation to the fine structure of starch remains to be explored. The *dull1* (*du1*) mutation, which results in dull, tarnished, and glassy mature kernels, is biochemically related to starch synthase III (SSIII).<sup>7,12</sup> So far, only one study on the influence of SSIII deficiency on the cluster and building-block structure of amylopectin from barley (*amo1* mutation) has been reported.<sup>13,14</sup> The interactions of the mutation type, the genetic background, and also the plant species determine the structure and functionalities of starch.<sup>6,15</sup> Comparing the fine structures of starches from *du1* maize and *amo1* barley mutants as influenced by SSIII deficiency thus provides an excellent opportunity to further understand these interactions.

The *du1* maize starch samples used in this research were from a previous report in which the genetics of mutants with a common genetic background (W64A) were described.<sup>16</sup> A previous study reported the molecular structures of amylose and amylopectin from the maize mutants.<sup>17</sup> It was shown that the structure of amylopectin was greatly altered by the mutation. The aim of this study was to further examine the influence of the *du1* mutation on the cluster and building block structures of amylopectin as affected by the SSIII deficiency. This study could contribute to a better understanding of the biosynthesis–structure relationships of starch in maize.

## MATERIALS AND METHODS

**Starches and Enzymes.** The maize samples, including one wild type (W64A) and three mutants from the same inbred genetic background, namely, two single *dull1* mutants (*du1-ref* and *du1-M3*) and one double *dull1-waxy* mutant (*du1-wx*), were the same specimens as used in previous studies.<sup>16,17</sup> A truncated enzyme protein was expressed at low level in *du1-ref* compared to the wild type, whereas no protein was produced in *du1-M3*. The *du1-wx* sample was essentially free of amylose. All of the *du1* mutations caused complete loss of SSIII enzyme activity. The exact locations of the mutations were given in a previous report.<sup>16</sup> Amylopectin from W64A, *du1-ref*, and *du1-M3* was isolated following the butanol–isoamyl alcohol precipitation method.<sup>18</sup> The purification procedure was repeated three times to ensure that the amylopectin fraction was free from amylose. The molecular structures of the starches were described in a previous report.<sup>17</sup>

Rabbit muscle phosphorylase *a* (EC 2.4.1.1, specific activity 22 U/mg) was obtained from Sigma (St. Louis, MO, USA).  $\alpha$ -Amylase of *Bacillus amyloliquefaciens* (EC 3.2.1.1),  $\beta$ -amylase of barley (EC 3.2.1.2, specific activity 705 U/mg), isoamylase of *Pseudomonas amyloclavata* (EC 3.2.1.68, specific activity 210 U/mg), and pullulanase of *Klebsiella pneumoniae* (EC 3.2.1.41, specific activity 699 U/mg) were obtained from Megazyme (Wicklow, Ireland). The activity of the  $\alpha$ -amylase (315 U/mL at pH 6.5, 25 °C) was determined based on a previous description.<sup>19</sup> The given activities of other enzymes were reported by the suppliers.

**Time-Course Analysis of  $\alpha$ -Amylolysis for Cluster Production from Amylopectin.** Amylopectin (20 mg) was dissolved in 400  $\mu$ L of 90% dimethyl sulfoxide (DMSO) by gentle heating and then constant stirring for one day at room temperature (~22 °C), before hot doubly distilled water (1.4 mL) was added. After the solution had been allowed to cool,  $\alpha$ -amylase (200  $\mu$ L, 0.9 U/mL) in NaOAc buffer (0.01 M, pH 6.5) was added to start the reaction in a water bath (25 °C) with magnetic stirring. The concentrations of substrate and  $\alpha$ -amylase in the reaction system were 10 mg/mL and 0.09 U/mL, respectively. Samples (200  $\mu$ L) were taken from 20 to 180 min. If a sample was not analyzed immediately, NaOH solution (4  $\mu$ L, 5.0 M) was added and mixed to destroy the  $\alpha$ -amylase, and then the sample was stored at –30 °C. Before analysis by gel permeation chromatography (GPC) on Sepharose CL 6B (as described below),

the sample was diluted in water (200  $\mu$ L) and conditioned by NaOH solution (40  $\mu$ L, 5.0 M).

**Production of  $\alpha$ -Dextrins and  $\varphi,\beta$ -Limit Dextrins of Clusters from Amylopectins.** Amylopectin (80 mg) was dissolved in 1.6 mL of 90% dimethyl sulfoxide (DMSO) by gentle heating and then constant stirring for one day at room temperature (~22 °C). Hot doubly distilled water (5.6 mL) was added, and after the mixture had been allowed to cool,  $\alpha$ -amylase (800  $\mu$ L, 0.9 U/mL) in NaOAc buffer (0.01 M, pH 6.5) was added to start the reaction in a water bath (25 °C) with magnetic stirring. The reaction was continued for 90 min before being stopped by adding NaOH (160  $\mu$ L, 5.0 M) and allowing the mixture to stand at room temperature for 2 h to destroy the  $\alpha$ -amylase. Methanol (40 mL) was added to precipitate the  $\alpha$ -dextrins of clusters. The sample was left at 4 °C for 3 h before the precipitate was recovered by centrifugation (4000g, 20 min) at room temperature. The precipitate was washed twice with methanol (10 mL) and allowed to stand in a fume hood to remove the methanol through evaporation.

The external chain segments of  $\alpha$ -dextrins of clusters were removed by phosphorylase *a* and  $\beta$ -amylase to obtain the  $\varphi,\beta$ -limit dextrins of clusters as previously described.<sup>20</sup> The solution of  $\varphi,\beta$ -LDs of clusters was stored at –30 °C before use.

**Production of Building Blocks from  $\varphi,\beta$ -Limit Dextrins of Clusters.** The carbohydrate content of  $\varphi,\beta$ -LDs of clusters in solution (10 mg) was adjusted by adding hot water, after which  $\alpha$ -amylase (60 U/mL) in NaOAc buffer (0.01 M, pH 6.5) was added at 35 °C to start the reaction, which then continued for 3 h to produce the building blocks. The concentrations of substrate and  $\alpha$ -amylase in the reaction system were 5 mg/mL and 6.0 U/mL, respectively. The reaction was stopped by boiling the mixture for 10 min. Then,  $\beta$ -amylase (5  $\mu$ L) with NaOAc buffer (pH 6.0, 0.01 M, 0.3 volume) was added to remove any remaining external chain segments. The  $\beta$ -amylolysis was conducted at 40 °C for 3 h before being stopped by boiling for 10 min. The building blocks in solution were stored at –30 °C before analysis.

**Debranching.** Solutions of clusters and building blocks (1 mg) were diluted in hot water (225  $\mu$ L). After the solutions had been allowed to cool, NaOAc buffer (25  $\mu$ L, 0.01 M, pH 5.5), pullulanase (1  $\mu$ L), and isoamylase (1  $\mu$ L) were added. The reaction was conducted at room temperature for 20 h with stirring to completely break the  $\alpha$ -(1,6) linkages before analysis by high-performance anion-exchange chromatography (HPAEC). The reaction was terminated by boiling for 10 min.

**Gel-Permeation Chromatography (GPC).** The clusters were analyzed on a column (1.6  $\times$  90 cm) of Sepharose CL 6B (Pharmacia, Uppsala, Sweden). The eluent was NaOH (0.5 M) with a pumping speed of 1.0 mL/min. The building blocks were analyzed on a column (1.6  $\times$  90 cm) of Superdex 30 (Pharmacia, Uppsala, Sweden) eluted with NaCl (0.05 M) at 1.0 mL/min. Fractions (1.0 mL) were analyzed for carbohydrate content by the phenol–sulfuric acid method.<sup>21</sup> The columns were calibrated with commercial linear dextrins of DP 1–7 (Supelco, Bellefonte, PA) and with branched dextrins of known DP (DP > 11) prepared from starch  $\alpha$ -amylase hydrolysates.<sup>22</sup>

**High-Performance Anion-Exchange Chromatography (HPAEC).** Samples were analyzed by high-performance anion-exchange chromatography with pulsed amperometric detection (HPAEC-PAD) on a Dionex ICS 3000 instrument (Sunnyvale, CA). The analytical column was CarboPac PA-100 (4  $\times$  250 mm), combined with a CarboPac PA-100 guard column (4  $\times$  50 mm). The flow rate was 1.0 mL/min, and the injection volume was 25  $\mu$ L, with a carbohydrate concentration of 1 mg/mL. The eluent phase consisted of solutions A (0.15 M NaOH) and B (0.15 M NaOH, containing 0.50 M NaOAc). The unit chain length distribution of debranched samples followed the gradient of eluent B: 0–9 min, 15–36%; 9–18 min, 36–45%; 18–110 min, 45–100% B. The composition of building blocks was analyzed using the following gradient: 0–15 min, 15–34%; 15–26 min, 34–40%; 26–52 min, 40–49%; 52–54 min, 49–100%. The column was equilibrated with 15% eluent B for 60 min between runs. Samples were diluted to fall into the linear range of response of the PAD detector, and the PAD signal was converted to carbohydrate content.<sup>23</sup> The PAD signals are comparable for branched and linear dextrins with the same DP.<sup>5</sup>

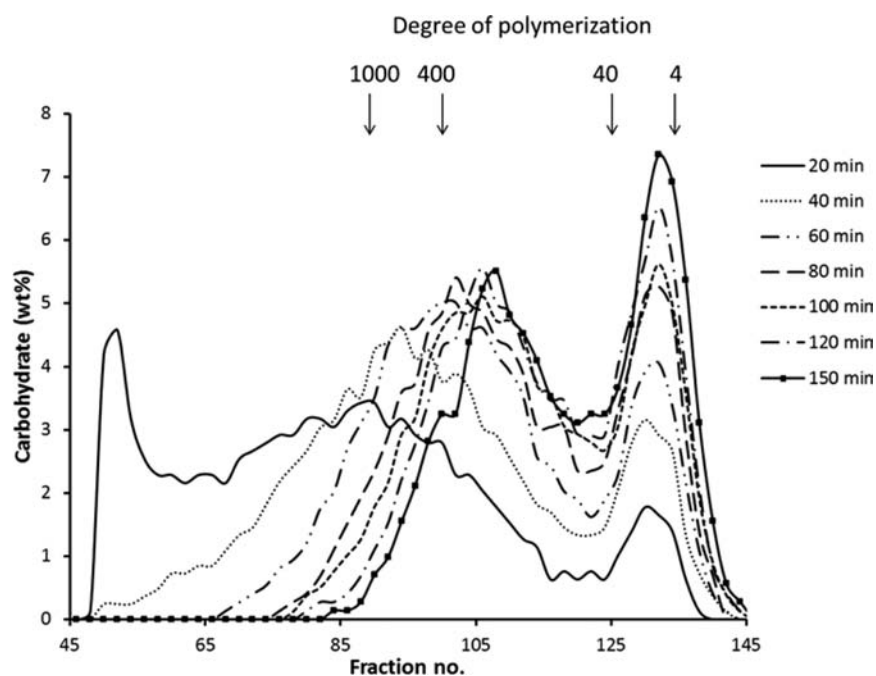


Figure 1. Time course of  $\alpha$ -amylolysis of amylopectins from W64A analyses by GPC on Sepharose CL 6B.

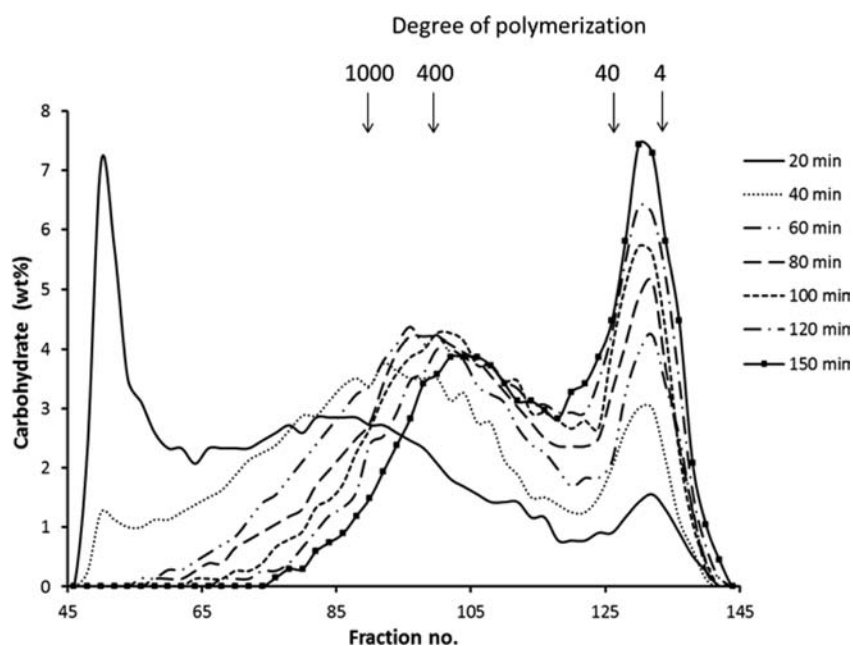


Figure 2. Time course of  $\alpha$ -amylolysis of amylopectins from *du1-M3* analyses by GPC on Sepharose CL 6B.

**Statistical Analysis.** Tests were conducted in triplicate and analyzed using SPSS version 19.0 software (IBM Corporation, Armonk, NY). Differences between means of data were compared by least significant difference at a significance level  $p < 0.05$ .

## RESULTS AND DISCUSSION

**Time-Course Analysis of  $\alpha$ -Amylolysis of Amylopectins.** The molecular weight distributions of the  $\alpha$ -amylolysates of all of the amylopectins, including wild type and *du1* mutants, had very similar patterns, with examples from W64A (Figure 1) and *du1-M3* (Figure 2) shown. Generally, all amylopectins, including mutant samples, from diverse botanical origins analyzed so far showed the same pattern of  $\alpha$ -amylolysis,<sup>1,13,20</sup>

which thus appears to be a universal feature according to the  $\alpha$ -amylase of *B. amyloliquefaciens*. The reaction was very fast in the initial stages, and branched dextrans with a wide range of molecular sizes (fractions 45–120) were produced. Within 20 min, domains containing groups of clusters were mainly produced. Dextrans with a peak at DP < 25 (fractions 120–145) represented mostly linear dextrans from the attack by the  $\alpha$ -amylase on external chains and possibly also the intercluster segments.<sup>24</sup> After 80 min, the reaction became slow as a result of hindrance from the branches in the clusters to  $\alpha$ -amylase action, and mostly clusters containing groups of building blocks were produced.<sup>4,5</sup> All *du1* mutant samples showed a similar pattern comparable with that of W64A. The average DP of

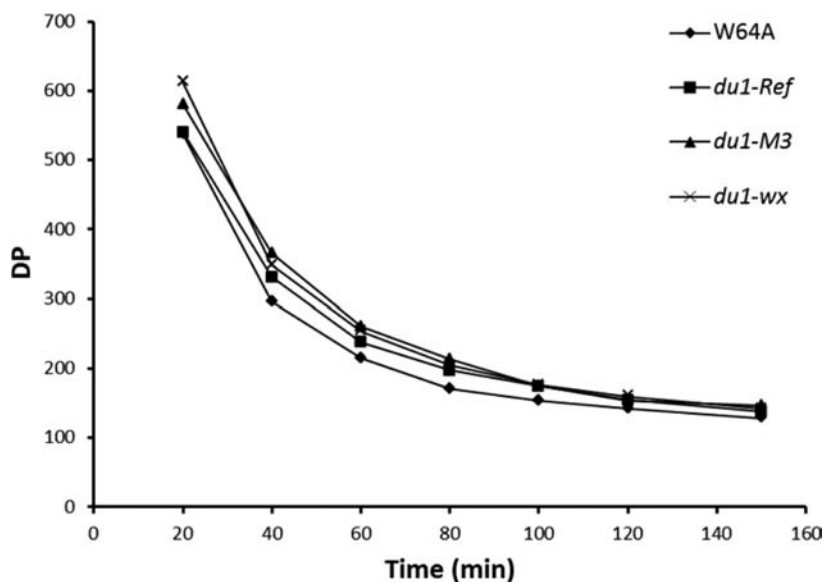


Figure 3. Development of average DP of branched dextrans as a function of time during the time course of  $\alpha$ -amylolysis of amylopectins.

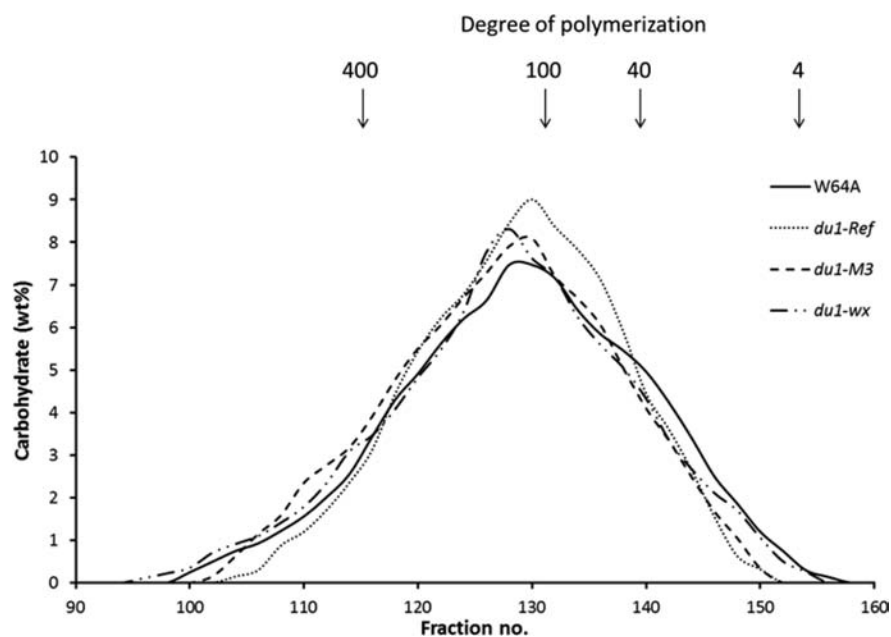


Figure 4. Molecular weight distribution obtained by GPC on Sepharose CL 6B of  $\varphi,\beta$ -limit dextrans of clusters.

branched dextrans (DP > 25) is plotted against time in Figure 3. Based on the time-course analysis, 90 min was chosen for cluster production on a preparative scale. The branched  $\alpha$ -dextrans representing clusters of branches were recovered by precipitation with methanol.

#### Characterization of $\varphi,\beta$ -Limit Dextrans of Clusters.

Only the internal part of clusters can be structurally compared between samples since the length of external chains left after  $\alpha$ -amylolysis is uneven. Thus  $\alpha$ -dextrans of clusters were further subjected to phosphorolysis and  $\beta$ -amylolysis to remove the remaining external chains. The molecular weight distributions of the  $\varphi,\beta$ -limit dextrans ( $\varphi,\beta$ -LDs) of clusters from different genotypes are shown in Figure 4. The peak DP for different genotypes was either 120 (W64A and *du1-wx*) or 140 (*du1-M3* and *du1-ref*). However, all *du1* mutants exhibited a higher average DP of their clusters than in W64A. In the amylose-free

double mutant *du1-wx*, the clusters had DP 80.6, and the values were even larger in the amylose-containing samples *du1-ref* (87.9) and *du1-M3* (88.1). In the nonmutant sample W64A, the DP was only 68.2. A previous study on the *amo1* mutation in barley, which results in SSIII deficiency, showed that *amo1* mutant samples also had larger cluster sizes.<sup>13</sup>

The samples of  $\varphi,\beta$ -LDs were debranched, and the internal unit chain length distributions were analyzed by HPAEC-PAD (Figure 5). With the combination of DP from GPC and chain length (CL) from HPAEC, diverse structural parameters (DB, degree of branching; NC, number of chains per cluster; ICL, internal chain length; TICL, total internal chain length) could be calculated (Table 1). DB was highest in the nonmutant sample (16.7%), and it was almost the same in *du1-wx*, whereas it was somewhat lower in *du1-ref* and *du1-M3*. Because of their larger cluster size, *du1* mutant samples also had higher NC

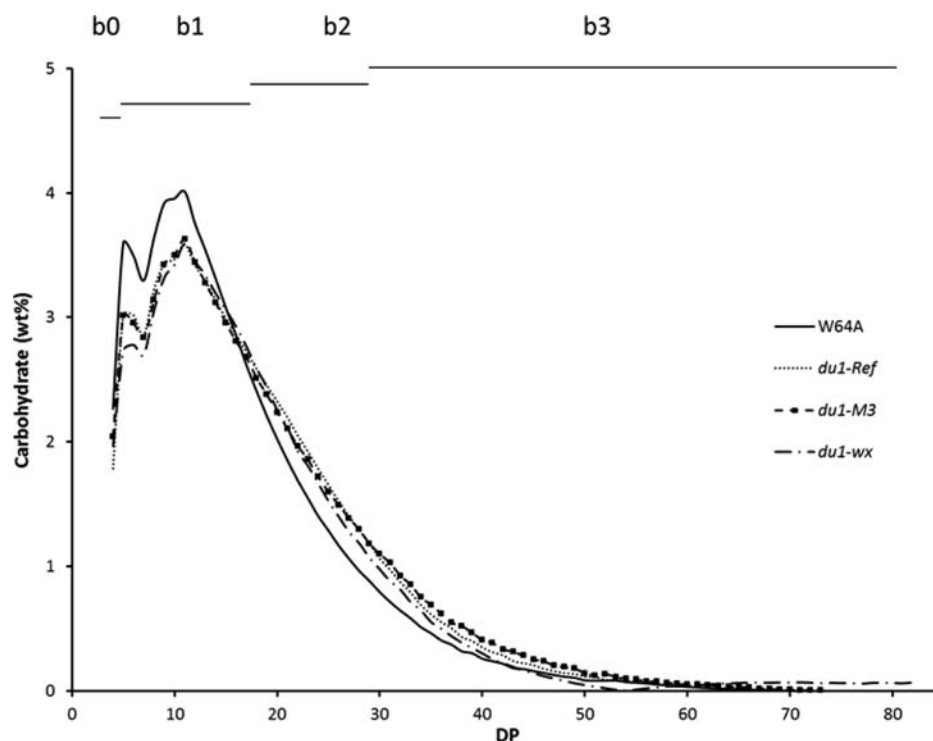


Figure 5. HPAEC fractionation of internal unit chain length distribution of  $\varphi,\beta$ -limit dextrins of clusters.

Table 1. Characterization of  $\varphi,\beta$ -Limit Dextrins of Clusters from Maize Amylopectins<sup>a</sup>

genotype	DP	NC	CL	ICL	TICL	DB
W64A	68.2 c	12.5 c	5.4 b	3.3 b	10.5 b	16.9 a
<i>du1-ref</i>	87.9 a	15.2 a	5.8 a	3.6 a	11.5 a	16.1 a
<i>du1-M3</i>	88.1 a	15.0 a	5.9 a	3.7 a	11.6 a	15.8 a
<i>du1-wx</i>	80.6 b	14.5 b	5.5 b	3.4 b	11.5 b	16.7 a

<sup>a</sup>DP, average degree of polymerization (DP) estimated by GPC; NC, number of chains estimated as DP/CL; CL, average chain length estimated by HPAEC; ICL, internal chain length =  $(CL - ECL) \times NC / (NC - 1) - 1$ , in which ECL is 1.5 for  $\varphi,\beta$ -limit dextrin; TICL, total internal chain length = CL of b-chains in  $\varphi,\beta$ -LD - 1; DB, degree of branching (%) =  $(NC - 1) / DP \times 100$ . Different lowercase letters within a column indicate significant differences ( $p < 0.05$ ).

values (14.5 for *du1-wx*, 15.2 for *du1-ref*, and 15.0 for *du1-M3*). Short chains (S-chains) in amylopectin were suggested to mostly participate in the formation of clusters, whereas long chains (L-chains) are involved in the interconnection of clusters.<sup>25</sup> A previous report showed that the SSIII deficiency resulted in a decrease of L-chains and an increase in S-chains in both whole amylopectin and its internal part in maize *du1* mutant samples.<sup>17</sup> The S/L molar ratios were 9.9 in W64A and 13.6, 14.1, and 13.7 in *du1-ref*, *du1-M3*, and *du1-wx*, respectively.<sup>17</sup> These values corresponded well with NC in the clusters, if it is assumed that NC in isolated clusters approximately equals S/L + 1.<sup>1</sup> In contrast, for example, isolated clusters from barley, rye, and oat had lower NC values than suggested by the S/L ratio in their amylopectins because some shorter chains were also involved in the interconnection of the clusters in those samples.<sup>1,13</sup> CLs of clusters from the single-mutant maize samples were 5.8–5.9, which was longer than that of W64A (5.4), whereas *du1-wx* had an only slightly elevated CL (5.5). CLs of clusters for all genotypes were shorter than those of their respective amylopectin  $\varphi,\beta$ -LDs

(~7.8).<sup>17</sup> A similar trend was observed for ICL and TICL. Interestingly, therefore, the larger size of the clusters in the mutants was associated not only with more chains in the clusters but also with longer internal chains. This result was different from that of a previous study on the *amo1* mutation in barley in which the clusters had TICLs similar to that of the nonmutant.<sup>13</sup>

In isolated clusters, new chains are formed when they are released from amylopectin by the  $\alpha$ -amylase. These chains were therefore designated by lowercase letters to be distinguished from the chain categories in amylopectin<sup>1</sup> and are illustrated in Figure 5. The profile of unit chain composition of clusters from all genotypes was rather similar, with peaks at DP 5 for b0-chains and at DP 11 for b1-chains. This was consistent with previous reports on this characteristic of the cluster structure of maize starches.<sup>1,26</sup> The molar composition of the diverse chain categories in the clusters is presented in Table 2. In the  $\varphi,\beta$ -LDs, a-chains appear as maltosyl residues.<sup>25</sup> However, in the clusters, some a-chains in the form of maltotriose also exist as a result of  $\alpha$ -amylase attack. The exact amount of a-chains can therefore not be determined. Nevertheless, the molar amount of a-chains in the form of maltose in all genotypes was rather

Table 2. Relative Molar Composition (%) of Chain Categories in  $\varphi,\beta$ -Limit Dextrins of Clusters from Maize Amylopectins<sup>a</sup>

genotype	a	DP 3	b0	b1	b2	b3
W64A	51.4 a	13.9 a	10.2 a	19.6 a	3.5 b	1.4 c
<i>du1-ref</i>	51.7 a	13.5 a	9.0 b	19.2 a	4.5 a	2.1 ab
<i>du1-M3</i>	52.5 a	11.8 b	9.5 b	19.4 a	4.4 a	2.3 a
<i>du1-wx</i>	53.4 a	14.2 a	8.3 c	18.2 c	4.1 a	1.8 b

<sup>a</sup>DP ranges of a = 2, b0 = 4–6, b1 = 7–18, b2 = 19–27, b3  $\geq$  28.<sup>1</sup> Chains at DP 3 are mixtures of a- and b-chains. Different lowercase letters within a column indicate significant differences ( $p < 0.05$ ).

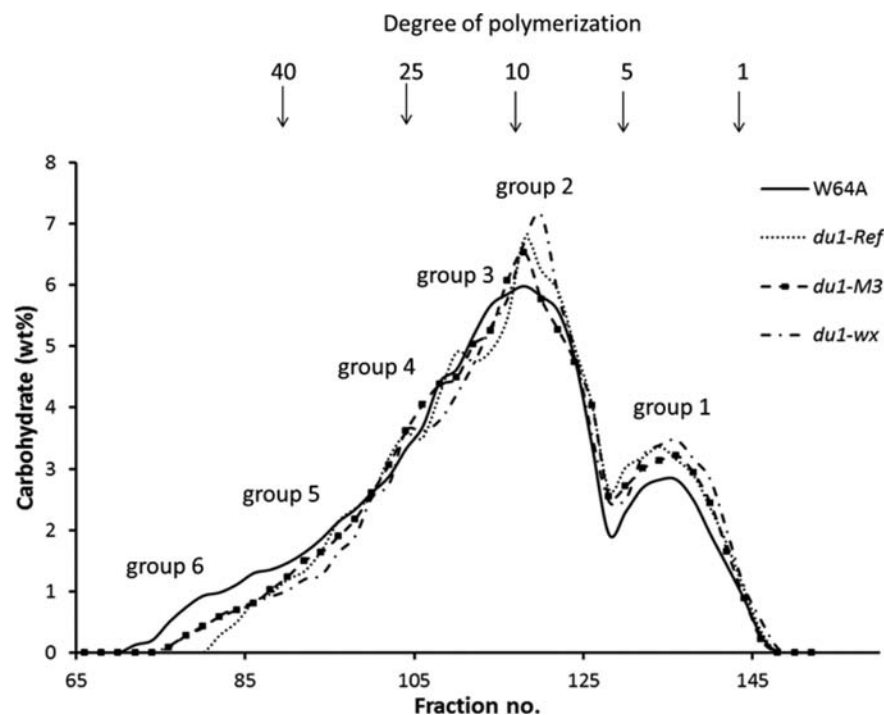


**Figure 6.** Fractionation of building blocks in clusters of maize amylopectins by GPC on Superdex 30.

similar (51.4–53.4%). The amount of chains at DP 3, which is a mixture of a-chains and the shortest b-chain,<sup>27</sup> greatly increased from ~2% in the amylopectins<sup>17</sup> to 13.5–14.2% in the clusters, with the exception of *du1-M3*, in which it was lower (11.8%). The *dull1* mutant samples had lower amounts of b0-chains (8.3–9.5%) and higher amounts of b2- (4.1–4.5%) and b3- (1.8–2.3%) chains compared with W64A (b0, 10.2%; b2, 3.5%; and b3, 1.4%). This result was unexpected, because the situation in the original amylopectins was the opposite, that is, S/L was higher in the mutants because of fewer long chains than in W64A. In contrast, it was previously reported that the *amo1* mutation in barley, which like *dull1* in maize has fewer long chains, results in clusters with decreased amounts of b2-chains.<sup>13</sup> This suggests different organizations of chains in the cluster structure in SSIII-deficient maize and barley mutant samples and is discussed in more detail below.

**Characterization of Building Blocks in Clusters.** The  $\varphi$ , $\beta$ -LDs of clusters were extensively hydrolyzed by a concentrated  $\alpha$ -amylase solution (6 U/mL) for 3 h and sequential  $\beta$ -amylolysis to reveal the composition of building blocks (practically  $\alpha$ -limit dextrins).<sup>28</sup> The molecular weight distribution of building blocks was analyzed by GPC on Superdex 30 (Figure 6) and HPAEC (Figures 7 and 8). All of the building blocks in clusters of amylopectins with different botanical origins produced by extensive hydrolysis with  $\alpha$ -amylase of *B. amyloliquefaciens* so far exhibited a similar general pattern.<sup>1</sup> It is therefore well-known that peak 1 in Figure 6 corresponds to glucose, maltose, and maltotriose (compare with Figure 7). The branched building blocks clearly consisted of four populations of dextrins (by relative weight) (P2–P5) with peak DP at 7, 11, 15, and 19, respectively (Figure 8), suggesting a nonrandom and systematic nature of branching in the clusters. The periodicity of building block size distribution in relation to the actual organization of chains in clusters remains to be explored. The branched building blocks have also been categorized into different groups (2–6) according to the

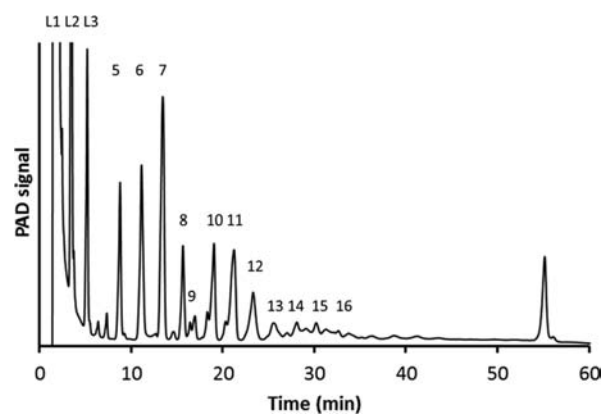


**Figure 7.** HPAEC chromatographs of building blocks from clusters of *du1-M3* amylopectin. Numbers show DP, and “L” denotes linear dextrins.

average number of chains per block.<sup>5</sup> The groups of two to four roughly correspond to the populations P2–P4 in terms of the DP boundary, whereas P5 corresponds to groups 5 and 6. The largest blocks in groups 5 and 6 were better distinguished by GPC (Figure 6). All of the building blocks analyzed so far from diverse botanical origins had the minimum-sized block at DP 5,<sup>2</sup> indicating a universal feature of amylopectin that can be revealed by  $\alpha$ -amylolysis.

The unit chain length composition of building blocks was also analyzed by HPAEC after debranching (Figure 9) and compared with the profile before debranching (Figure 7) to reveal the branching pattern of the blocks in the clusters. With the combination of GPC and HPAEC data, various structural parameters of building blocks could be calculated (Table 3). As expected, compared to clusters and amylopectins, the tightly branched building blocks had much smaller DP, CL, ICL, and TICL values and thus higher DB values. The linear fraction (DP 1–3) in the building block mixture is produced by the  $\alpha$ -

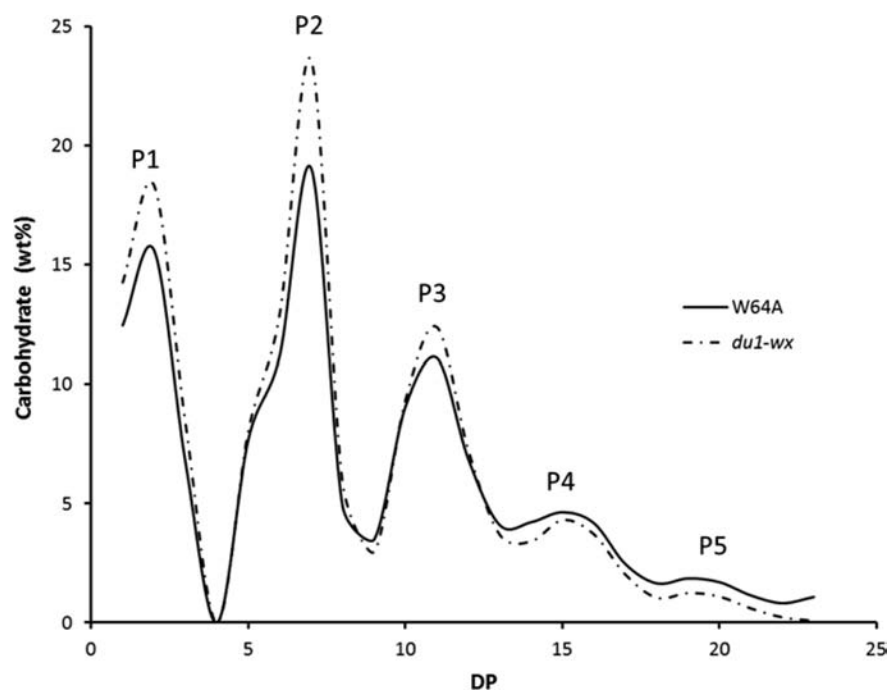


**Figure 8.** Fractionation of building blocks in clusters of maize amylopectins by HPAEC. P1–P5 represent distinguishable dextrin populations by weight of 1–5, respectively. P1 indicates the population of linear dextrans, and P2–P5 indicate the populations of branched dextrans. DP 4 does not exist in the building block mixtures.

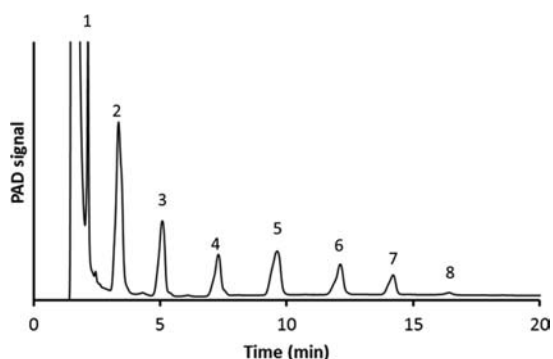


**Figure 9.** HPAEC chromatograms of debranched building blocks from clusters of *du1-M3* amylopectin. Numbers show DP.

amylase from interblock segments in the clusters.<sup>5</sup> W64A had a lower relative molar content of linear dextrans (47.9%) compared with *dull1* mutant samples (50.2–54.3%). As a result, W64A had a higher proportion of branched building blocks than the *dull1* mutant samples. The building blocks from W64A also had a higher average DP (12.1) and a higher

average number of chains per block (NC, 3.3) than the *dull1* mutant samples (DP, 11.2–11.4; NC, 3.0–3.1). However, the chain length values (CL, ICL, and TICL) were similar in all genotypes. The general features of building blocks from all genotypes in this study were comparable with those of previous reports on building blocks from amylopectins from diverse botanical origins.<sup>1,2,9</sup>

From the structural differences between clusters and their building blocks, the average composition of building blocks in clusters was calculated (Table 4). The average interblock chain length (IB-CL), reflecting the interconnection of building blocks in clusters<sup>30</sup> and shown to be related to functional properties of starch,<sup>31</sup> can be estimated from the amount of the small linear fragments relative to the amount of branched dextrans.<sup>32</sup> All maize genotypes had similar IB-CL values (6.2–6.5). W64A had a lower number of blocks per cluster (NBbl) (4.2) than the mutant samples, of which *du1-wx* had a lower NBbl (5.2) than *du1-ref* and *du1-M3* (5.5–5.6), which can be attributed to the smaller cluster size (Table 1). This, in turn, resulted in a somewhat lower density of blocks (DBbl) for W64A (6.1). The relative distributions of the different groups of building blocks in the clusters are also summarized in Table

**Table 3.** Characterization of Building Blocks in  $\alpha$ , $\beta$ -Limit Dextrans of Clusters from Maize Amylopectins<sup>a</sup>

genotype	linear		branched							
	mol %	DP	wt %	mol %	DP	CL	ICL	TICL	NC	DB
W64A	47.9 c	2.2 a	86.0 a	52.1 a	12.1 a	3.7 a	1.5 a	4.2 a	3.3 a	18.8 a
<i>du1-ref</i>	50.8 b	2.1 a	83.5 b	49.2 b	11.2 b	3.7 a	1.5 a	4.1 a	3.0 b	18.2 a
<i>du1-M3</i>	50.2 b	2.2 a	84.0 b	49.7 b	11.4 b	3.7 a	1.4 a	4.1 a	3.1 b	18.6 a
<i>du1-wx</i>	54.3 a	2.1 a	81.9 c	45.7 c	11.2 b	3.7 a	1.5 a	4.2 a	3.0 b	18.2 a

<sup>a</sup>Linear dextrans have DP 1, 2, and 3, and branched building blocks have DP  $\geq$  5. DP, average DP estimated by GPC; CL, average chain length estimated by HPAEC; ICL, internal chain length =  $(CL - ECL) \times NC / (NC - 1) - 1$ , in which external chain length (ECL) is estimated as 2; TICL, total internal chain length; NC, number of chains =  $DP / CL$ ; DB, degree of branching (%) =  $(N - 1) \times 100 / DP$ . Different lowercase letters within a column indicate significant differences ( $p < 0.05$ ).

**Table 4. Composition of Building Blocks in  $\phi,\beta$ -Limit Dextrins of Clusters from Maize Amylopectins<sup>a</sup>**

genotype	distribution of block categories (mol %)						
	IB-CL	DBbl	NBbl	group 2	group 3	group 4	groups 5 and 6
W64A	6.2 b	6.1 b	4.2 c	51.1 c	27.0 a	10.4 a	11.4 a
<i>du1-ref</i>	6.2 b	6.4 a	5.6 a	55.3 a	24.8 c	9.7 ab	10.1 bc
<i>du1-M3</i>	6.2 b	6.3 a	5.5 a	53.1 b	26.4 a	10.1 a	10.3 b
<i>du1-wx</i>	6.5 a	6.4 a	5.2 b	55.1 a	26.2 a	9.2 b	9.5 c

<sup>a</sup>IB-CL, interblock chain length per cluster = (mol %)<sub>linear</sub> × DP<sub>linear</sub> / (mol %)<sub>branched</sub> + 4; DBbl, density of building blocks per cluster = NBbl/DP<sub>ctr</sub> × 100, in which DP<sub>ctr</sub> is the average DP of  $\phi,\beta$ -LDs of clusters; NBbl, number of building blocks per cluster = (wt %)<sub>Bbl</sub> / 100 × DP<sub>cluster</sub> / DP<sub>Bbl</sub> in which (wt %)<sub>Bbl</sub> is the weight percentage of branched building blocks. Categorization of groups 2–6 of building blocks based on their numbers of chains per block. Different lowercase letters within a column indicate significant differences ( $p < 0.05$ )

4. In general, the distributions of diverse groups of building blocks from different genotypes were within the range of the results on maize amylopectin previously reported.<sup>1</sup> Among different genotypes, W64A had a lower amount of group 2 (51.1%) and a higher amount of groups 5 and 6 (11.4%) than the *dull1* mutant samples (group 2, 53.1–55.3%; groups 5 and 6, 9.2–10.1%), whereas all of the genotypes had similar amounts of groups 3 and 4. Interestingly, the previous study on the *amo1* mutant samples showed that SSIII deficiency in the barley resulted in the opposite change, namely, an increased amount of building blocks of groups 5 and 6 and a decreased amount of building blocks of group 2 compared with the wild type.<sup>14</sup> This can be attributed to a difference in plant species. Among the *dull1* mutant samples analyzed here, minor structural differences on the building block level were also noted, further supporting the structural observations on the cluster and amylopectin levels as discussed above and previously.<sup>17</sup> Thus, the genetics of mutation should be carefully documented in relation to the amylopectin structure in mutant samples.

#### Effect of SSIII Deficiency on Cluster Structure in *du1* and *amo1* Mutants of Maize and Barley, Respectively

Previously, systematic studies on amylopectin from nonmutant plants revealed some general features. Structural correlations exist between the cluster structure in diverse plants and their respective amylopectins,<sup>1,2</sup> the latter of which are categorized into four different groups based on their internal structure.<sup>3</sup> One example is that the amount of long B-chains in amylopectin is positively related to the amount of longer b-chains in clusters and also to the interblock chain length (IB-CL).

The cluster structure of amylopectin can be interpreted by the backbone model proposed previously,<sup>1,2</sup> in which the building blocks and clusters are connected by a backbone. The longer b-chains in the clusters serve as the backbone, and shorter chains, including a-chains and short b-chains, participate in building-block formation. The backbone might be provided with a few or more side chains that also carry building blocks. Most, if not all, of the intercluster segments (which are longer than IB-CL) appear, however, to be found along the actual backbone.<sup>33</sup> Small differences in this general structure give rise to amylopectins with typical cluster features. According to the present model,<sup>1</sup> a backbone with few side chains tends to be found in amylopectins with more L-chains and small clusters with more b2- and b3-chains, whereas more extensively

branched backbones are found in amylopectins with few L-chains and large clusters with few b2- and b3-chains. Maize, which is a type 2 amylopectin, is predicted to have a slightly less branched backbone than barley, which is a type 1 amylopectin.<sup>3</sup> It is therefore interesting to consider how the cluster structure of SSIII-deficient mutants possibly fits into this general picture.

As noted above, some partly contradictory features and differences appear to exist between the *du1* mutant maize samples analyzed here and the *amo1* mutant barley samples analyzed previously.<sup>13,14</sup> In both cases, the long chains of amylopectin are reduced in relative number, and the short chains therefore are more abundant. However, whereas both the internal and external structures are affected in the *du1* mutation,<sup>17</sup> in the *amo1* mutant, only the internal structure is altered and the external structure remains similar to that of nonmutant barley.<sup>13</sup> On the cluster level, both mutations result in larger clusters, but for different reasons. In *amo1* mutant barley, the clusters have more a-chains and the short b-chains because of an increased number of large building blocks of groups 5 and 6 (consisting of five chains or more). In contrast, the large cluster size in *du1* mutant maize is due to a higher number of the longer b2- and b3-chains (Figure 5) and more of the smallest building blocks with only two chains, whereas fewer large blocks of groups 5 and 6 are present (Figure 6). Furthermore, although the length of the internal segments was shorter in the amylopectin of both mutant types, the internal segments in *du1* mutant clusters were longer than in the nonmutant clusters (ICL and TICL, Table 1), whereas in *amo1* mutant clusters, the internal segments were similar to those in nonmutant clusters.

A possible explanation for these apparently partly contradictory results might be found on the basis of the backbone concept. From the values given in Tables 1 and 2, the number of chains in a typical *du1* cluster is given in Table 5 as the

**Table 5. Theoretical Composition of Chains in  $\phi,\beta$ -Limit Dextrins of Clusters from *du1* and *amo1* Mutants of Maize and Barley in Comparison with Their Wild Types<sup>a</sup>**

sample	NC	a	DP 3	b0	b1	b2	b3
Maize							
W64A	12.5	6.4	1.7	1.3	2.5	0.4	0.2
<i>du1</i>	15.1	7.9	1.9	1.4	2.9	0.7	0.3
NC <sub>excess</sub>	2.6	1.5	0.2	0.1	0.4	0.3	0.1
NC <sub>excess</sub> (%)	100	54.5	9.1	6.1	18.2	9.1	3.0
Barley							
nonmutant	12.3	6.0	1.2	1.4	3.0	0.5	0.2
<i>amo1</i>	17.1	7.8	1.8	2.3	4.3	0.6	0.3
NC <sub>excess</sub>	4.8	1.8	0.6	0.9	1.3	0.1	0.1
NC <sub>excess</sub> (%)	100	37.5	12.5	18.7	27.1	2.1	2.1

<sup>a</sup>Values are based on the molar composition given in Table 2 for W64A, and those for *du1* are average values for *du1-ref* and *du1-M3*. Values for barley starches are based on values given for cluster fractions IL2 and IL3 by Bertoft et al.<sup>13</sup> DP range of a = 2, b0 = 4–6, b1 = 7–18, b2 = 19–27, b3 ≥ 28.<sup>1</sup> DP 3 is an unknown mixture of a- and b-chains.

average of *du1-ref* and *du1-M3* (selected because they exhibited a more pronounced difference from W64A than *du1-wx*) and compared with the value for the nonmutant. The total increase in the number of chains in the clusters of the mutants was 2.6. On a relative basis, it was calculated that around 54% of these chains were a-chains (in the form of maltose) and the rest were



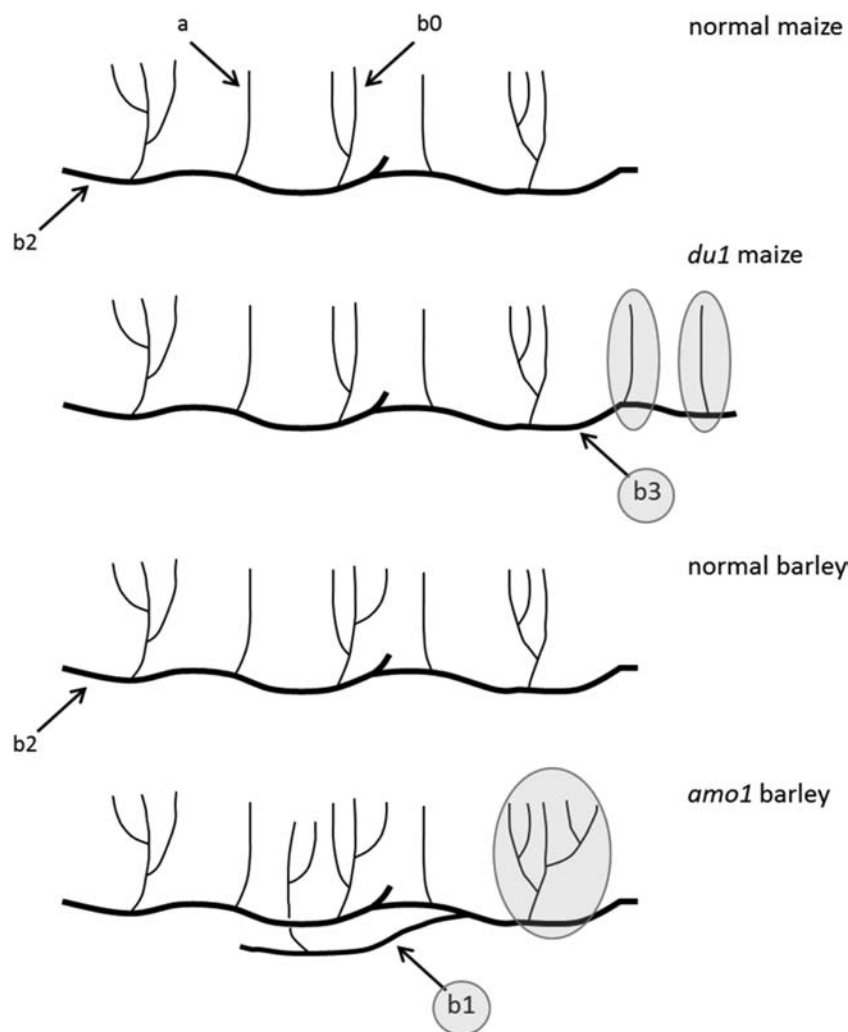


**Figure 10.** Schematic showing the principle differences of the structure of clusters in normal and SSIII-deficient mutants of maize and barley amylopectins. Chains mainly comprising the backbone (bold lines) and chains forming building blocks (thin lines), together with their definition and nomenclature in clusters, are indicated. b0-chains are inside building blocks, and b1-, b2-, and b3-chains contain one, two, and three interblock segments interconnecting two, three, and four building blocks, respectively. The *du1* mutation in maize results in more a-chains and long b-chains (b2- and b3-chains) and more of the smallest building blocks (circled) along the backbone. The *amo1* mutation in barley results in more short b-chains, of which b0-chains increase the number of large building blocks (circled) and b1-chains mainly constitute new branches to the backbone.

distributed among the b-chain categories (Table 5). These values were compared with the large clusters of *amo1* mutants and clusters of nonmutants of barley reported by Bertoft et al.<sup>13</sup> In the mutant barley, the proportion of additional a-chains and longer b-chains in the enlarged clusters was clearly less pronounced than that in the maize mutants, whereas the shorter b-chains increased more in barley than in maize. Of the short b-chains, b0-chains are found inside building blocks, and b1-chains contain one interblock segment (and thus connect two building blocks) and might to a significant degree represent the branch chains of the backbone. The longer b2- and b3-chains, however, contain two or more such segments and are probably more common along the backbone of amylopectin.<sup>1</sup> Thus, this provides a clue to the principal differences in the cluster structures of maize and barley. Although a single picture of a cluster cannot represent the complicated mixture of the vast variations in individual clusters that probably exist in reality, general principles of the structural changes can be envisioned, and schematic representations of these aspects are presented in Figure 10. Compared to the nonmutant maize (W64A), the larger *du1* mutant cluster has more of the small

building blocks of group 2 (circled) along the backbone. This results in more of the longer b-chains, which are distributed preferentially along the backbone. It also results in proportionally more interblock chain segments, which would be the reason for the greater average ICL and TICL values. In contrast, the larger clusters of *amo1* mutant barley are due to more large building blocks and more side chains along the backbone (in the form of b1-chains). This change in the structure compared to that of nonmutant barley does not necessarily affect ICL and TICL.

The differences depicted here between maize and barley are, of course, due to two different mutations that have a deficiency of SSIII in common, but are probably also due to altered levels of other enzymes of biosynthesis, as shown previously in maize and other plant species.<sup>9–11,34</sup> It is likely, however, that comparable differences can also be found between *du1* mutants of maize with different genetic backgrounds, as it has been shown that the unit chain profiles are different in different inbred lines.<sup>15</sup> In addition, it has been shown that the properties of *du1* maize mutants with diverse genetic backgrounds are significantly different.<sup>6</sup> Thus, it appears that

this investigation is only an initial step toward a full understanding of the biosynthetic effects obtained as a result of SSIII deficiency in plants of diverse species and of diverse genetic backgrounds within species.

In conclusion, *dull1* mutation greatly affected the cluster and building-block structure of maize amylopectin. The *dull1* mutation resulted in larger clusters by DP  $\approx$  20 in the form of  $\varphi$ , $\beta$ -limit dextrans. Clusters of *dull1* mutants had more chains per cluster and also greater chain lengths, internal chain lengths, and total internal chain lengths than in the wild type. The *dull1* mutation resulted in a decrease in the amount of b0-chains (DP 4–6) and an increase in the numbers of b2- and b3-chains (DP  $\geq$  19). Furthermore, the *dull1* mutation created more of the smallest branched building blocks with two chains, resulting in more building blocks in the clusters, but without altering the average internal structure of the blocks. Within clusters, all of the genotypes had similar IB-CL values. The type of *dull1* mutation (*du1-ref*, *du1-M3*, or *du1-wx*) influenced specific features of the cluster and building-block structures and was different from the *amo1* mutation in barley, which also exhibits deficient SSIII activity. The backbone model of amylopectin can explain the organization of building blocks in clusters altered by the SSIII deficiency.

## AUTHOR INFORMATION

### Corresponding Author

\*E-mail: kseethar@umn.edu.

### Notes

The authors declare no competing financial interest.

## ACKNOWLEDGMENTS

Maize starch samples were kindly provided by Professor Alan M. Myers at Department of Biochemistry, Biophysics, and Molecular Biology, Iowa State University, Ames, IA. Technical assistance on amylopectin isolation from Miss Anna Källman at the Department of Food Science, Swedish University of Agricultural Sciences, Uppsala, Sweden, is gratefully appreciated.

## REFERENCES

- (1) Bertoft, E.; Koch, K.; Åman, P. Building block organisation of clusters in amylopectin from different structural types. *Int. J. Biol. Macromol.* **2012**, *50*, 1212–1223.
- (2) Bertoft, E.; Koch, K.; Åman, P. Structure of building blocks in amylopectins. *Carbohydr. Res.* **2012**, *361*, 105–113.
- (3) Bertoft, E.; Piyachomkwan, K.; Chatakanonda, P.; Sriroth, K. Internal unit chain composition in amylopectins. *Carbohydr. Polym.* **2008**, *74*, 527–543.
- (4) Bertoft, E. The use of alpha-amylase in structural studies of amylopectin. Ph.D. Thesis, Åbo Akademi, Åbo, Finland, 1990.
- (5) Bertoft, E. Composition of building blocks in clusters from potato amylopectin. *Carbohydr. Polym.* **2007**, *70*, 123–136.
- (6) Li, J.; Corke, H. Physicochemical properties of maize starches expressing dull and sugary-2 mutants in different genetic backgrounds. *J. Agric. Food Chem.* **1999**, *47*, 4939–4943.
- (7) Keeling, P. L.; Myers, A. M. Biochemistry and genetics of starch synthesis. *Annu. Rev. Food Sci. Technol.* **2010**, *1*, 271–303.
- (8) Kötting, O.; Kossmann, J.; Zeeman, S. C.; Lloyd, J. R. Regulation of starch metabolism: The age of enlightenment? *Curr. Opin. Plant Biol.* **2010**, *13*, 321–329.
- (9) Singletary, G. W.; Banisadr, W.; Keeling, P. L. Influence of gene dosage on carbohydrate synthesis and enzymatic activities in endosperm of starch-deficient mutants of maize. *Plant Physiol.* **1997**, *113*, 293–304.
- (10) Cao, H.; Imparl-Radosevich, J.; Guan, H.; Keeling, P. L.; James, M. G.; Myers, A. M. Identification of the soluble starch synthase activities of maize endosperm. *Plant Physiol.* **1999**, *120*, 205–215.
- (11) Szydłowski, N.; Ragel, P.; Hennen-Bierwagen, T. A.; Planchot, V.; Myers, A. M.; Mérida, A.; d'Hulst, C.; Wattebled, F. Integrated functions among multiple starch synthases determine both amylopectin chain length and branch linkage location in *Arabidopsis* leaf starch. *J. Exp. Bot.* **2011**, *62*, 4547–4559.
- (12) Gao, M.; Wanat, J.; Stinard, P. S.; James, M. G.; Myers, A. M. Characterization of *dull1*, a maize gene coding for a novel starch synthase. *Plant Cell* **1998**, *10*, 399–412.
- (13) Bertoft, E.; Källman, A.; Koch, K.; Andersson, R.; Åman, P. The cluster structure of barley amylopectins of different genetic backgrounds. *Int. J. Biol. Macromol.* **2011**, *49*, 441–453.
- (14) Bertoft, E.; Källman, A.; Koch, K.; Andersson, R.; Åman, P. The building block structure of barley amylopectin. *Int. J. Biol. Macromol.* **2011**, *49*, 900–909.
- (15) Boyer, C. D.; Liu, K. C. The interaction of endosperm genotype and genetic background. Part 1. Differences in chromatographic profiles of starches from nonmutant and mutant endosperms. *Starch/Stärke* **1985**, *37*, 73–79.
- (16) Lin, Q.; Huang, B.; Zhang, M.; Zhang, X.; Rivenbark, J.; Lappe, R. L.; James, M. G.; Myers, A. M.; Hennen-Bierwagen, T. A. Functional interactions between starch synthase III and isoamylase-type starch-debranching enzyme in maize endosperm. *Plant Physiol.* **2012**, *158*, 679–692.
- (17) Zhu, F.; Bertoft, E.; Källman, A.; Myers, A. M.; Seetharaman, K. Molecular structure of starches from maize mutants deficient in starch synthase III. *J. Agric. Food Chem.* **2013**, *61*, 9899–9907.
- (18) Klucinec, J. D.; Thompson, D. B. Fractionation of high-amylose maize starches by differential alcohol precipitation and chromatography of the fractions. *Cereal Chem.* **1998**, *75*, 887–896.
- (19) Bertoft, E.; Manelius, R.; Qin, Z. Studies on the structure of pea starches. Part 1: Initial stages in  $\alpha$ -amylolysis of granular smooth pea starch. *Starch/Stärke* **1993**, *45*, 215–220.
- (20) Zhu, F.; Corke, H.; Åman, P.; Bertoft, E. Structures of clusters in sweetpotato amylopectin. *Carbohydr. Res.* **2011**, *346*, 1112–1121.
- (21) Dubois, M.; Gilles, K. A.; Hamilton, J. K.; Rebers, P. A.; Smith, F. Colorimetric method for determination of sugars and related substances. *Anal. Chem.* **1956**, *28*, 350–356.
- (22) Bertoft, E.; Spoo, L. Fractional precipitation of amylopectin alpha-dextrans using methanol. *Carbohydr. Res.* **1989**, *189*, 169–180.
- (23) Koch, K.; Andersson, R.; Åman, P. Quantitative analysis of amylopectin unit chains by means of high-performance anion-exchange chromatography with pulsed amperometric detection. *J. Chromatogr. A* **1998**, *800*, 199–206.
- (24) Bertoft, E. Composition of clusters and their arrangement in potato amylopectin. *Carbohydr. Polym.* **2007**, *68*, 433–446.
- (25) Bertoft, E. On the nature of categories of chains in amylopectin and their connection to the super helix model. *Carbohydr. Polym.* **2004**, *57*, 211–224.
- (26) Zhu, F.; Bertoft, E.; Seetharaman, K. Characterization of internal structure of maize starch without amylose and amylopectin separation. *Carbohydr. Polym.* **2013**, *97*, 475–481.
- (27) Bertoft, E.; Koch, K. Composition of chains in waxy-rice starch and its structural units. *Carbohydr. Polym.* **2000**, *41*, 121–132.
- (28) Zhu, F.; Corke, H.; Åman, P.; Bertoft, E. Structures of building blocks in clusters of sweetpotato amylopectin. *Carbohydr. Res.* **2011**, *346*, 2913–2925.
- (29) Umeki, K.; Yamamoto, T. Structures of branched dextrans produced by saccharifying  $\alpha$ -amylase of *Bacillus subtilis*. *J. Biochem.* **1972**, *72*, 1219–1226.
- (30) Kong, X.; Corke, H.; Bertoft, E. Fine structure characterization of amylopectins from grain amaranth starch. *Carbohydr. Res.* **2009**, *344*, 1701–1708.
- (31) Vamadevan, V.; Bertoft, E.; Seetharaman, K. On the importance of organization of glucan chains on thermal properties of starch. *Carbohydr. Polym.* **2013**, *92*, 1653–1659.

(32) Bertoft, E.; Laohaphatanalert, K.; Piyachomkwan, K.; Sriroth, K. The fine structure of cassava starch amylopectin. Part 2: Building block structure of clusters. *Int. J. Biol. Macromol.* **2010**, *47*, 325–335.

(33) Källman, A.; Bertoft, E.; Koch, K.; Åman, P.; Andersson, R. On the interconnection of clusters and building blocks in barley amylopectin. *Int. J. Biol. Macromol.* **2013**, *55*, 75–82.

(34) Fujita, N.; Yoshida, M.; Kondo, T.; Saito, K.; Utsumi, Y.; Tokunaga, T.; Nishi, A.; Satoh, H.; Park, J. H.; Jane, J. L.; Miyao, A.; Hirochika, H.; Nakamura, Y. Characterization of SSIIIa-deficient mutants of rice: The function of SSIIIa and pleiotropic effects by SSIIIa deficiency in the rice endosperm. *Plant Physiol.* **2007**, *144*, 2009–2023.